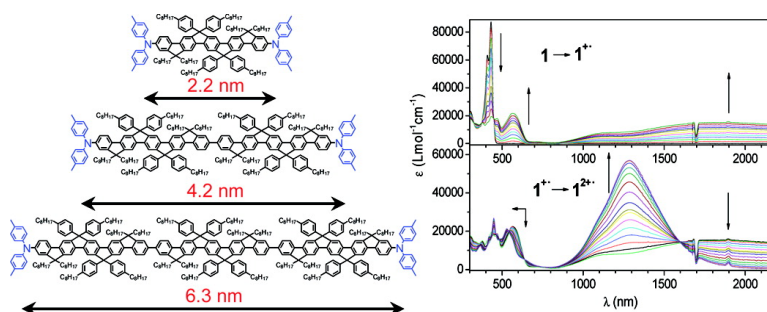


Arylamine-Substituted Oligo(ladder-type pentaphenylene)s: Electronic Communication between Bridged Redox Centers

Gang Zhou, Martin Baumgarten, and Klaus Müllen

J. Am. Chem. Soc., **2007**, 129 (40), 12211-12221 • DOI: 10.1021/ja073148s • Publication Date (Web): 19 September 2007

Downloaded from <http://pubs.acs.org> on February 14, 2009



More About This Article

Additional resources and features associated with this article are available within the HTML version:

- Supporting Information
- Links to the 9 articles that cite this article, as of the time of this article download
- Access to high resolution figures
- Links to articles and content related to this article
- Copyright permission to reproduce figures and/or text from this article

[View the Full Text HTML](#)

Arylamine-Substituted Oligo(ladder-type pentaphenylene)s: Electronic Communication between Bridged Redox Centers

Gang Zhou, Martin Baumgarten, and Klaus Müllen*

Contribution from the Max-Planck-Institute for Polymer Research, Ackermannweg 10, D-55128 Mainz, Germany

Received May 4, 2007; E-mail: muellen@mpip-mainz.mpg.de

Abstract: Novel bis(arylamine-substituted) oligo(ladder-type pentaphenylene)s **1–3**, with bridge lengths estimated to be 2.2, 4.2, and 6.3 nm, respectively, have been developed, and the model compound **4** with a mono-arylamine substituent was also synthesized. Their absorption spectra in different solvents are almost identical, while distinct bathochromic shifts of the photoluminescence (PL) spectra were observed with increasing solvent polarity due to the polarized excited states. The cyclic voltammetry (CV) and differential pulse voltammetry (DPV) spectra display a two-step oxidation of the bridged diamines in compound **1**, which suggests that the electron and charge delocalize in mixed-valence (MV) cation **1⁺** and that both redox centers can communicate through the pentaphenylene bridge. Only unresolved curves in CV and DPV spectra were observed in the first two oxidation processes of diamines **2** and **3**, indicating that the bridges are too long for efficient delocalization over the entire molecules and the radical cations localize at each arylamine center. This finding was further supported by chemical oxidation with SbCl_5 and studies of the corresponding UV–vis–NIR absorption spectra of compounds **1–4**. A significant intervalence charge-transfer (IVCT) band around 5283 cm^{-1} (1893 nm) was observed in **1⁺**. This is the first report of such a highly intense IVCT band in the NIR region with intensity similar to that of the visible band of the radicals, enabling further analysis of the CT process and the coupling matrix element V , classifying **1⁺** as a class II derivative ($V = 1.6\text{ kcal/mol}$). This study may offer an effective way to improve the understanding of charge transfer and charge-carrier transport in various conjugated oligomers or polymers and facilitate their ongoing exploration in optoelectronic applications.

Introduction

Conjugated organic oligomers and polymers are widely investigated in view of their optoelectronic and biological applications, such as light-emitting diodes (LEDs),¹ photovoltaic devices,² field-effect transistors (FETs),³ nonlinear optics,⁴ and chemical and biological sensors.⁵ Of those, phenylene-based π -conjugated systems are the most important class of conjugated materials for electronic applications due to their efficient blue emission.⁶ In particular, *p*-phenylene,⁷ fluorene,⁸ indenofluorene,⁹ phenanthrylene,¹⁰ and ladder-type¹¹ phenylene-based oligomers and polymers have been developed as efficient LED materials. To achieve better hole-transport, triarylaminines are

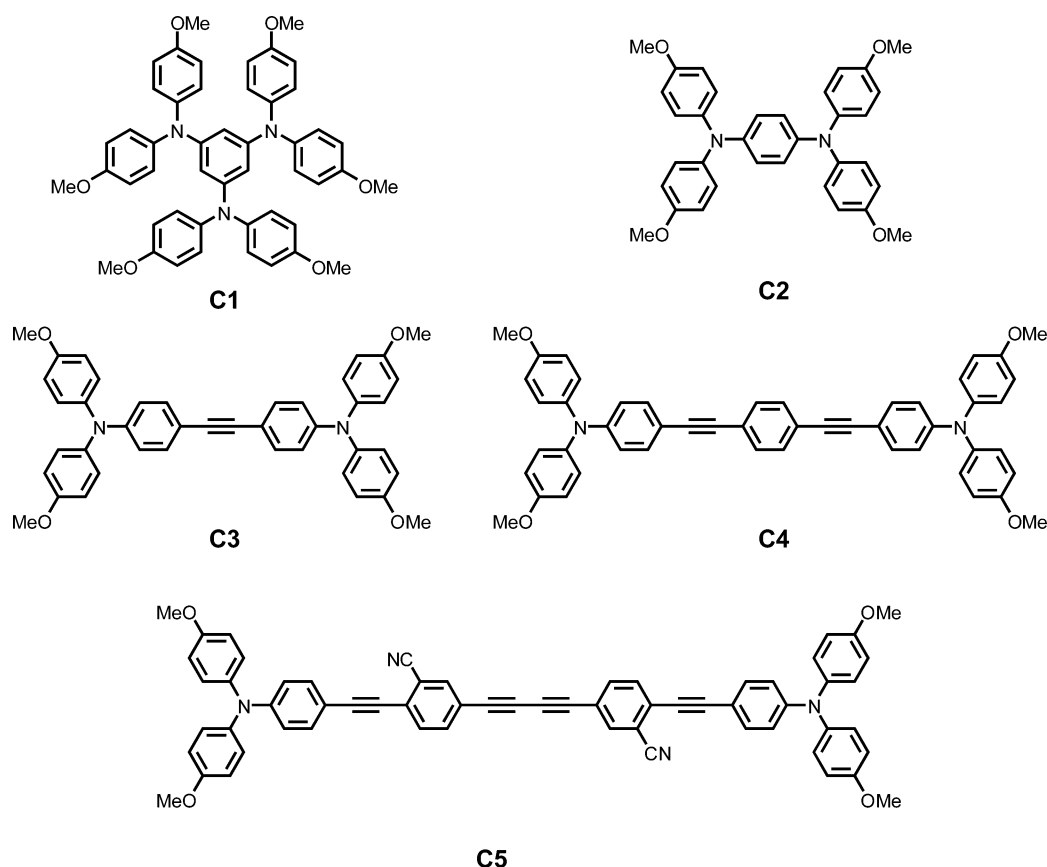
introduced because of their ability to transport positive charge via their radical cations.¹²

Purely organic mixed-valence (MV) cations have received increasing attention since they provide the simplest models for the investigation of basic electron-transfer (ET) and charge-transfer (CT) processes.¹³ Usually, the most essential organic MV systems are complexes in which two organic redox centers with different oxidation states are connected by saturated or unsaturated bridges, where the two corresponding valence structures are $\text{R}^{+\cdot}\text{-bridge-R}$ and $\text{R-bridge-R}^{+\cdot}$ (R is the redox center).¹⁴ Among the numerous redox groups, bis-

- (1) Müller, C. D.; Falcou, A.; Reckefuss, N.; Rojahn, M.; Wiederhorn, V.; Rudati, P.; Frohne, H.; Nuyken, O.; Becker, H.; Meerholz, K. *Nature* **2003**, *421*, 829.
- (2) Wohrle, D.; Meissner, D. *Adv. Mater.* **1991**, *3*, 129.
- (3) Bao, Z.; Lovinger, A. J.; Brown, J. J. *Am. Chem. Soc.* **1998**, *120*, 207.
- (4) Williams, D. J. *Angew. Chem., Int. Ed. Engl.* **1984**, *23*, 640.
- (5) Swager, T. M. *Acc. Chem. Res.* **1998**, *31*, 201.
- (6) Kraft, A.; Grimsdale, A. C.; Holmes, A. B. *Angew. Chem., Int. Ed.* **1998**, *37*, 402.
- (7) Remmers, M.; Neher, D.; Grüner, J.; Friend, R. H.; Gelinck, G. H.; Warman, J. M.; Quattrocchi, C.; dos Santos, D. A.; Brédas, J.-L. *Macromolecules* **1996**, *29*, 7432.
- (8) Leclerc, M. J. *Polym. Sci. A: Polym. Chem.* **2001**, *39*, 2867.
- (9) Setayesh, S.; Marsitzky, D.; Müllen, K. *Macromolecules* **2000**, *33*, 2016.
- (10) Yang, C.; Scheiber, H.; List, E. J. W.; Jacob, J. Müllen, K. *Macromolecules* **2006**, *39*, 5213.
- (11) Scherf, U. *J. Mater. Chem.* **1999**, *9*, 1853.

- (12) Thelakkat, M. *Macromol. Mater. Eng.* **2002**, *287*, 442.
- (13) (a) Coropceanu, V.; Gruhn, N. E.; Barlow, S.; Lambart, C.; Durivage, J. C.; Bill, T. G.; Nöll, G.; Marder, S. R.; Brédas, J.-L. *J. Am. Chem. Soc.* **2004**, *126*, 272. (b) Brunshwig, B. S.; Creutz, C.; Sutin, N. *Chem. Soc. Rev.* **2002**, *31*, 168. (c) Launay, J.-P. *Chem. Soc. Rev.* **2001**, *30*, 386. (d) Baumgarten, M.; Huber, W.; Müllen, K. *Advances in Physical Organic Chemistry*; Academic Press: London, 1993; Vol. 28, p 1. (e) Nelsen, S. F. *Chem. Eur. J.* **2000**, *6*, 581. (f) Sporer, C.; Ratera, I.; Ruiz-Molina, D.; Zhao, Y.; Vidal-Gancedo, J.; Wurst, K.; Jaitner, P.; Clays, K.; Persoons, A.; Rovira, C.; Veciana, J. *Angew. Chem., Int. Ed.* **2004**, *43*, 5266. (g) Heckmann, A.; Lambert, C.; Goebel, M.; Wortmann, R. *Angew. Chem., Int. Ed.* **2004**, *43*, 5851. (h) Nelsen, S. F.; Ismagilov, R. F.; Trieber, D. A. *Science* **1997**, *278*, 846. (i) D'Alessandro, D. M.; Topley, A. C.; Davies, M. S.; Keene, F. R. *Chem. Eur. J.* **2006**, *12*, 4873. (j) Nelsen, S. F.; Ismagilov, R. F.; Powell, D. R. *J. Am. Chem. Soc.* **1996**, *118*, 6313. (k) Nelsen, S. F.; Ismagilov, R. F.; Powell, D. R. *J. Am. Chem. Soc.* **1997**, *119*, 10213. (l) Nelsen, S. F.; Ismagilov, R. F.; Powell, D. R. *J. Am. Chem. Soc.* **1998**, *120*, 1924. (m) Nelsen, S. F.; Ismagilov, R. F.; Gentile, K. E.; Powell, D. R. *J. Am. Chem. Soc.* **1999**, *121*, 7108. (n) Nelsen, S. F.; Trieber, D. A.; Ismagilov, R. F.; Teki, Y. *J. Am. Chem. Soc.* **2001**, *123*, 5684.
- (14) Richardson, D. E.; Taube, H. *Coord. Chem. Rev.* **1984**, *60*, 107.

Chart 1



triarylamines are of great interest in studying hole-transfer processes from one redox center to the other¹⁵ because triarylamines are widely used as hole-conducting materials in LEDs,¹⁶ photovoltaic cells,¹⁷ photorefractive materials for optical data storage,¹⁸ electrochromic polymers,¹⁹ and xerographic processes.²⁰ In general, there are a number of advantages in utilizing triarylamines in MV compounds.²¹ First, triarylamines guarantee reversible redox behavior as long as the para-positions of the phenyl rings are protected. This stability is due to the delocalization of the positive charge and the spin within the triarylamine moiety.²² Second, the spacer between the two triarylamine redox centers can be varied over a broad range very easily. Third, the intervalence charge-transfer (IVCT) band associated with optically induced hole transfer from one triarylamine center to the

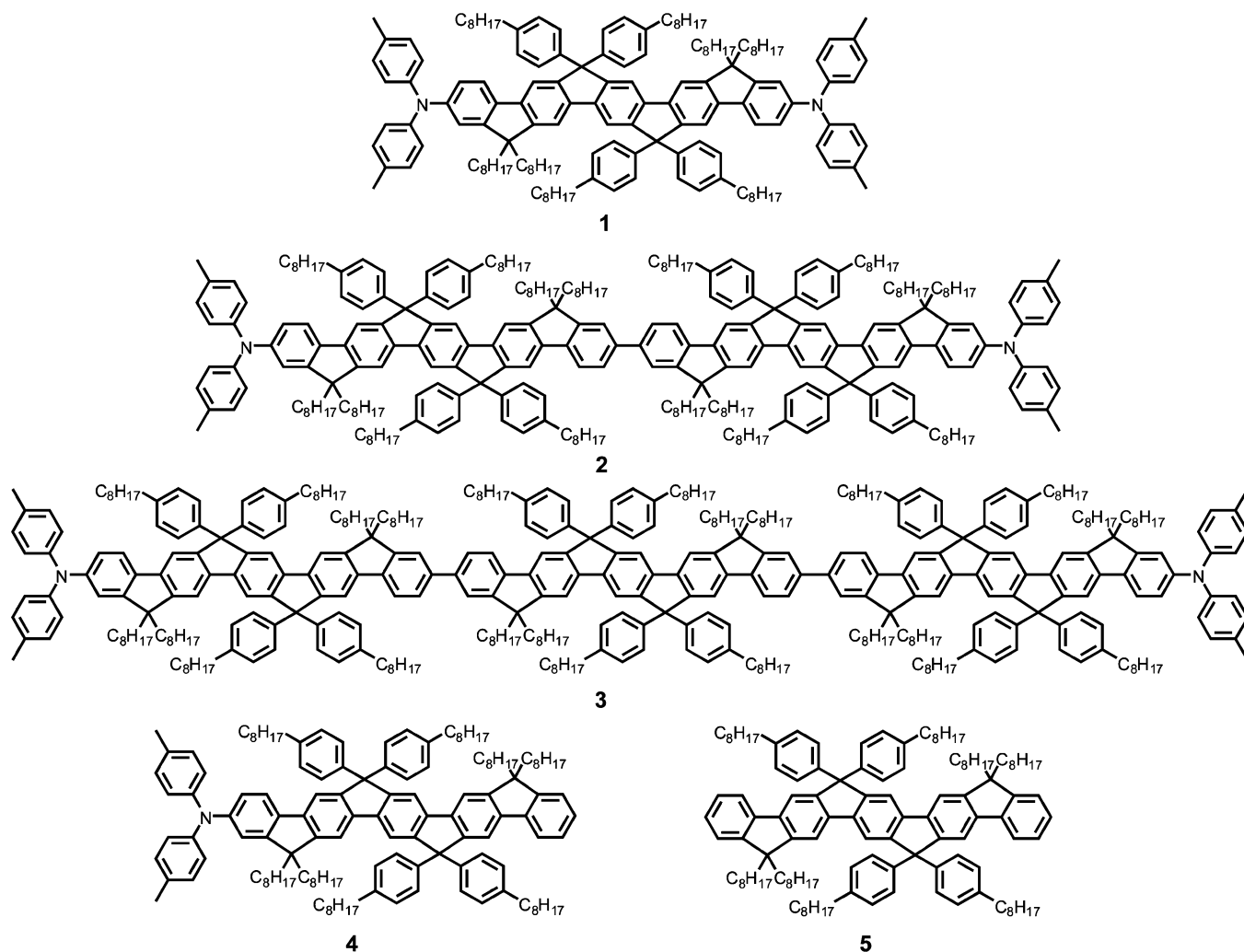
other is usually quite intense and well separated from other bands so as to allow accurate band fits. Fourth, the redox potentials of the triarylamine centers can be tuned by substituents in the para-position.²³

In early research, Stickley et al.²⁴ investigated the simplest MV compounds with phenylene as spacer and triarylamine as redox center, such as compound **C1** (Chart 1), and discovered the solution-stable monocationic, dicationic, and tricationic states of *N,N,N',N'',N''',N''''*-hexaphenyl/hexaanisyl-1,3,5-triaminobenzene. Lambert et al.²⁵ extended the bridge of organic MV compounds to *p*-phenylene and *p*-phenylene ethynylene systems (**C2**–**C4**), with spacer distances varying from 0.5 to 2 nm, and found that the electronic coupling integral decreased with increasing spacer distance. Heckmann et al.²⁶ then built up a 2.87 nm spacer (**C5**) with electron-deficient cyano groups to raise the energy of the bridge state and observed the IVCT along with a rather weak electronic interaction. However, although a lot of conjugated bridges with long distance have been designed and their IVCT properties investigated, most of the spacer backbones were not planar due to the torsion about formal single bonds, which may weaken the π -conjugation in the molecules. Herein, a planar and better conjugated spacer, ladder-type pentaphenylene, was used to bridge the two redox centers. In order to combine the good hole-transport of triarylamines with efficient blue luminescence of oligopentaphenylenes, a set of three novel bis(arylamine-substituted) oligo(ladder-type pen-

- (15) (a) Bonvoisin, J.; Launay, J.-P. *J. Phys. Chem.* **1994**, *98*, 5052. (b) Lambert, C.; Nöll, G.; Schelter, J. *Nat. Mater.* **2002**, *1*, 69. (c) Szeghalmi, A.; Erdmann, M.; Engel, V.; Schmitt, M.; Amthor, S.; Kriegisch, V.; Nöll, G.; Rainer, S.; Lambert, C.; Leusser, D.; Stalke, D.; Zabel, M.; Popp, J. *J. Am. Chem. Soc.* **2004**, *126*, 7834. (d) Wu, J.; Baumgarten, M.; Debije, M. G.; Warman, J. M.; Müllen, K. *Angew. Chem., Int. Ed.* **2004**, *43*, 5331. (e) Nishiumi, T.; Nomura, Y.; Chimoto, Y.; Higuchi, M.; Yamamoto, K. *J. Phys. Chem. B* **2004**, *108*, 7992. (f) Coropceanu, V.; Malagoli, M.; André, J. M.; Brédas, J. L. *J. Am. Chem. Soc.* **2002**, *124*, 10519. (g) Bonvoisin, J.; Launay, J.-P.; Verbouwe, W.; Van der Auweraer, M.; de Schryver, F. C. *J. Phys. Chem.* **1996**, *100*, 17079. (h) Bonvoisin, J.; Launay, J.-P.; Rovira, C.; Veciana, J. *Angew. Chem.* **1994**, *106*, 2190; *Angew. Chem., Int. Ed. Engl.* **1994**, *33*, 2106. (i) Lambert, C.; Schelter, J.; Fiebig, T.; Mank, D.; Trifonov, A. *J. Am. Chem. Soc.* **2005**, *127*, 10600. (16) Scherf, U.; List, E. J. W. *Adv. Mater.* **2002**, *14*, 477. (17) Cremer, J.; Bäuerle, P.; Wienk, M. M.; Janssen, R. A. J. *Chem. Mater.* **2006**, *18*, 5832. (18) Moerner, W. E.; Silence, S. M. *Chem. Rev.* **1994**, *94*, 127. (19) Nishikitani, Y.; Kobayashi, M.; Uchida, S.; Kubo, T. *Electrochim. Acta* **2001**, *46*, 2035. (20) Bender, T. P.; Graham, J. F.; Duff, J. M. *Chem. Mater.* **2001**, *13*, 4105. (21) Lambert, C.; Nöll, G. *J. Chem. Soc., Perkin Trans. 2* **2002**, 2039. (22) Neugebauer, F. A.; Bamberger, S.; Groh, W. R. *Chem. Ber.* **1975**, *108*, 2406.

- (23) Dapperheld, S.; Steckhan, E.; Brinkhaus, K.-H. G.; Esch, T. *Chem. Ber.* **1991**, *124*, 2557. (24) Stickley, K. R.; Blackstock, S. C. *J. Am. Chem. Soc.* **1994**, *116*, 11576. (25) Lambert, C.; Nöll, G. *J. Am. Chem. Soc.* **1999**, *121*, 8434. (26) Heckmann, A.; Amthor, S.; Lambert, C. *Chem. Commun.* **2006**, 2959.

Chart 2



taphenylene), **1–3** (Chart 2), was designed and synthesized, with spacer lengths estimated to be 2.2, 4.3, and 6.3 nm, respectively. Model compounds **4**, with a monoarylamine substituent, and **5**, with no arylamine substituent, were also prepared for comparison. Their IVCT behaviors among the spacer and the two redox centers were investigated by means of cyclic voltammetry, differential pulse voltammetry, and chemical oxidation monitored by UV–vis–NIR absorption spectra. It is believed that the in-depth characterization of the oxidative formation of radical cations and higher charged states provides further insight into the intramolecular charge transfer and charge-carrier transport in this kind of conjugated oligomers and polymers.

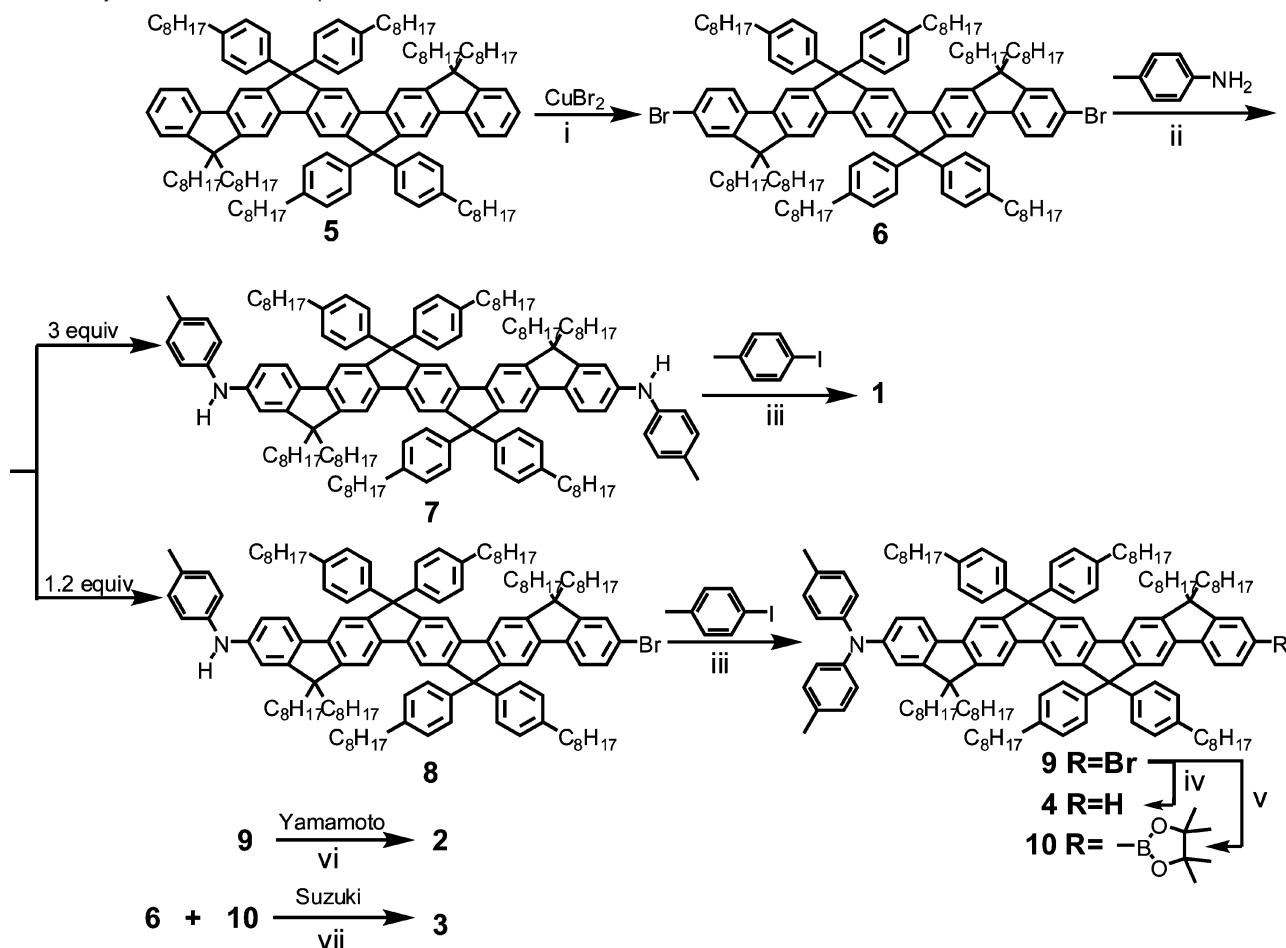
Results and Discussion

Synthesis and Structure Characterization. The synthetic approach to compounds **1–4** is depicted in Scheme 1. It started from alkyl- and aryl-substituted ladder-type pentaphenylene **5**, which was previously developed in our laboratory.²⁷ Compound **5** was easily converted into the corresponding dibromopentaphenylene **6** (91%) by bromination with copper bromide on alumina in carbon tetrachloride. Our further synthesis of

arylamine-substituted ladder-type pentaphenylene materials by direct Buchwald coupling of brominated pentaphenylene with diphenylamine is not applicable because the attachment of diphenylamine to the bulky pentaphenylene does not bring a remarkable change to the polarity of pentaphenylene and it is not straightforward to separate the mixture of non-, mono- and bis(arylamine-substituted) pentaphenylenes. An alternative two-step approach begins with a Buchwald coupling of primary anilines with aryl bromides, followed by an Ullmann-type reaction carried out by arylation of the secondary amine with aryl iodide. In this work, a modified Buchwald coupling²⁸ of bromide **6** and 3 equiv of *p*-toluidine with palladium acetate as catalyst in toluene generated the symmetrical secondary amine **7** (85%), which was purified by chromatography on silica gel with dichloromethane/hexane = 1/15 as eluent. An Ullmann-type reaction²⁹ was then carried out by refluxing amine **7** with *p*-iodotoluene in toluene. This gave the corresponding tertiary amine, diamine **1** (70%), which was chromatographed on silica gel with cyclohexane as eluent. The *p*-methyl substituents were chosen to ensure reversible oxidation of the arylamine groups and clear assignments of the aryl hydrogen in the 1H NMR spectrum.

(27) Jacob, J.; Sax, S.; Piok, T.; List, E. J. W.; Grimsdale, A. C.; Müllen, K. J. *Am. Chem. Soc.* **2004**, *126*, 6987.

(28) Sadighi, J. P.; Harris, M. C.; Buchwald, S. L. *Tetrahedron Lett.* **1998**, *39*, 5327.

Scheme 1. Synthetic Route of Compounds 1–3^a

^a Reagents and conditions: (i) $\text{CuBr}_2/\text{alumina}$, CCl_4 , 90°C , 16 h; (ii) *p*-toluidine, $\text{Pd}(\text{OAc})_2$, bis[2-(diphenylphosphino)phenyl] ether, *t*- $\text{C}_4\text{H}_9\text{Na}$, toluene, 80°C , 8 h; (iii) *p*-iodotoluene, 1,10-phenanthroline, CuCl , KOH , toluene, 140°C , 24 h; (iv) *n*- BuLi , -78°C , H_2O , room temperature, 4 h; (v) *n*- BuLi , -78°C , 2-isopropoxy-4,4,5,5-tetramethyl-1,3,2-dioxaborolane, room temperature, 24 h; (vi) $\text{Ni}(\text{COD})$, bipyridine, COD , DMF , toluene, 80°C , 48 h; (vii) $\text{Pd}(\text{PPh}_3)_4$, K_2CO_3 , toluene, H_2O , 80°C , 48 h.

When bromide **6** was treated with 1.2 equiv of *p*-toluidine as shown above, the asymmetrically substituted secondary arylamine **8** was obtained with a yield of 35% and then transformed via an Ullmann-type reaction to the corresponding tertiary arylamine **9** (83%). A nickel(0)-mediated Yamamoto coupling³⁰ of compound **9** produced the crude diamine **2**, and after chromatography on silica gel with cyclohexane as eluent, the pure product was obtained with a yield of 74%.

Addition of *n*-butyllithium to the solution of compound **9** in tetrahydrofuran and quenching with water afforded model compound **4** (93%). Lithiation of compound **9** with *n*-butyllithium, followed by addition of 2-isopropoxy-4,4,5,5-tetramethyl-1,3,2-dioxaborolane, produced the corresponding boronate ester **10** (29%). The diamine **3** was then synthesized by Suzuki coupling³¹ of **6** and **10** with $\text{Pd}(\text{PPh}_3)_4$ as catalyst and purified by chromatography on silica gel with cyclohexane as eluent in 49% yield.

The structures of diamines **1–3** are validated by comparing the integration of the singlet peaks at $\delta = 2.2$ ppm and triplet peaks at $\delta = 2.5$ ppm in the ^1H NMR spectra, which are attributed to the *p*-methyl protons of the bis(*p*-tolyl)amine units

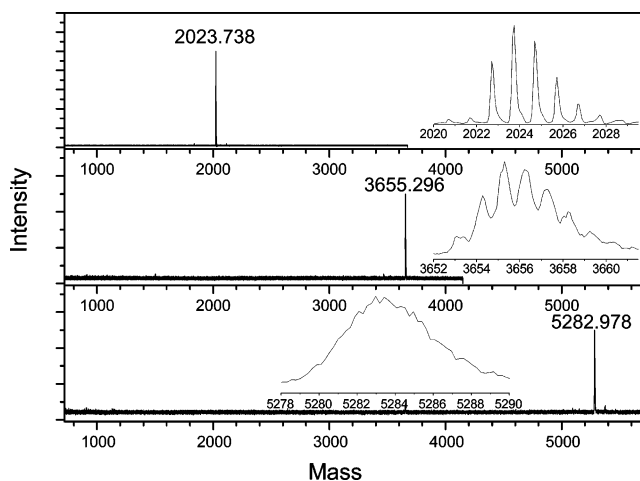


Figure 1. MALDI-TOF MS spectra of diamines 1–3.

and the α -protons of the *p*-octylphenylene close to the bridging methylene (9-position of fluorene) units, respectively. In addition to ^1H NMR and ^{13}C NMR spectroscopic and elemental analysis evidence, MALDI-TOF mass spectra exhibited single intense signals corresponding to the calculated masses of compounds **1–3**, as illustrated in Figure 1, together with an expanded view of the molecular-ion region.

(29) Zhang, Q.; Chen, J.; Cheng, Y.; Wang, L.; Ma, D.; Jing, X.; Wang, F. *J. Mater. Chem.* **2004**, *14*, 895.

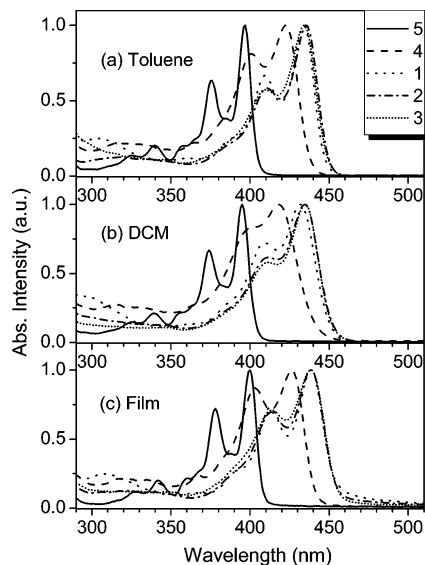
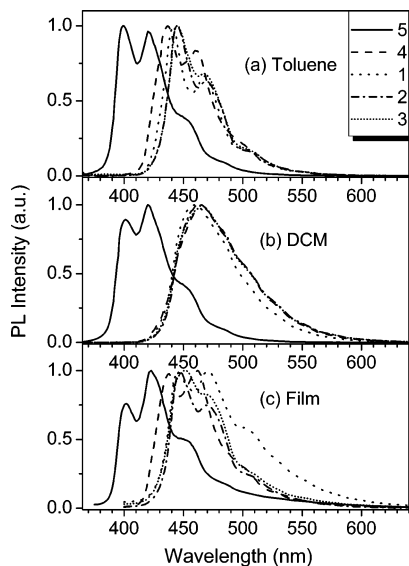
(30) Yamamoto, T. *Macromol. Rapid. Commun.* **2002**, *23*, 583.

(31) Miyaura, N.; Suzuki, A. *Chem. Rev.* **1995**, *95*, 2457.

Table 1. Optical Data of Compounds 1–5

compd	toluene solution ^a			dichloromethane solution ^a			film	
	$\lambda_{\text{max}}^{\text{Abs}}$ (nm)	$\lambda_{\text{max}}^{\text{PL}}$ (nm) ^b	$\Phi_{\text{PL}}^{\text{c}}$	$\lambda_{\text{max}}^{\text{Abs}}$ (nm)	$\lambda_{\text{max}}^{\text{PL}}$ (nm) ^b	$\Phi_{\text{PL}}^{\text{c}}$	$\lambda_{\text{max}}^{\text{Abs}}$ (nm)	$\lambda_{\text{max}}^{\text{PL}}$ (nm) ^b
1	409, 434	441, 468	0.81	409, 432	465	0.84	413, 439	446, 471
2	411, 435	444, 469	0.82	411, 435	465	0.76	413, 439	447, 469
3	411, 435	445, 466	0.81	411, 435	465	0.76	413, 439	452, 469
4	401, 423	437, 460	0.82	401, 418	460	0.71	403, 426	438, 462
5	376, 397	399, 420	0.79	374, 395	401, 420	0.62	378, 400	402, 423

^a Measured in solution with a concentration of 5×10^{-6} M. ^b Excited at 355 nm. ^c Fluorescence quantum yield measured relative to 9,10-diphenylanthracene.³⁶

**Figure 2.** Absorption spectra of compounds 1–5 in toluene and dichloromethane solutions and in solid states.**Figure 3.** Photoluminescence spectra of compounds 1–5 in toluene and dichloromethane solutions and in solid states.

Optical Properties. Compounds 1–5 are soluble in common organic solvents, such as toluene, dichloromethane, and chloroform. The optical absorption (Figure 2) and photoluminescence (PL) (Figure 3) spectra in different solutions were measured at a concentration of ca. 5×10^{-6} M, and the results are summarized in Table 1. As shown in Figure 2a, stepwise incorporation of pentaphenylene with bis(*p*-tolyl)amine from compounds 5 to 4 and from 4 to 1 induces 26 and 11 nm bathochromic shifts, respectively, due to the extended conjugation. However, the increase in the number of pentaphenylene

units from one to three leads only to negligible shifts of the absorption spectra upon going from 1 to 2 and from 2 to 3. This indicates that the conjugation of the pentaphenylene backbone no longer extends over two pentaphenylene units,²⁷ unlike typical oligofluorene systems, where the effective conjugation length reaches the maximum in the 16-mer.³² One plausible explanation is that the pentaphenylene-substituted arylamine groups are stronger electron donors than the pentaphenylene groups themselves and have a higher impact on the bathochromic shift of optical absorption than the extension of the number of pentaphenylene units themselves. Thereby the effect of conjugation length extension is minimized. The corresponding PL spectra of compounds 1–5 in toluene solutions demonstrate two resolved emission bands which are symmetrical to the absorption spectra and assigned to the 0–0 and 0–1 singlet transitions (Figure 3a).³³ The absorption and PL spectra of compounds 1–5 in dichloromethane solutions were also investigated. As shown in Figure 2b, the absorption maxima of compounds 1–5 in dichloromethane solutions are not significantly distinct from those in toluene solutions. In contrast, the differences in the PL spectra between dichloromethane solutions and toluene solutions are more remarkable, except for model compound 5 without an arylamine unit. The PL spectra of compounds 1–4 in dichloromethane solutions display a 20–24 nm bathochromic shift of the maximum intensity compared with those in toluene solutions. In addition, the resolution of vibrational modes in the PL spectra completely disappeared, and only one intense broad signal was left. Since no aggregation absorption or excimer emission was observed, we attribute this bathochromic shift to a polarized excited state.³⁴ Due to the electron transition from the highest occupied molecular orbital (HOMO), localized primarily on the arylamine moieties, to the lowest unoccupied molecular orbital (LUMO), localized on the pentaphenylene moieties, upon excitation, a dipole is created in the excited S_1 state, much larger than that of the ground state. Dichloromethane is a more polar solvent than toluene and therefore is able to stabilize this polarized excited state by the reorientation of the solvent molecules to accommodate the increased dipole, lowering the energy of the system, which induced the even further bathochromic shift of the PL spectrum of compound 1 in *N,N*-dimethylformamide (DMF) solution ($\lambda_{\text{max}} = 467$ nm). The absence of aggregation is also evidenced by the relatively high fluorescence quantum yield (Φ) of diamines 1–3 in dichloromethane solutions ($\geq 76\%$, shown in Table 1). This phenomenon of solvent relaxation and the accompanying increase in Stokes shift with increasing solvent polarity were also investigated in other donor-substituted π -bridged systems, where the π -system acts as an acceptor.³⁵

(32) Geng, Y.; Trajkovska, A.; Katsis, D.; Ou, J. J.; Culligan, S. W.; Chen, S. *J. Am. Chem. Soc.* **2002**, *124*, 8337.

(33) Valeur, B. *Molecular Fluorescence*; Wiley-VCH: Weinheim, 2002.

(34) Clarke, T. M.; Gordon, K. C.; Kwok, W. M.; Phillips, D. L.; Officer, D. L. *J. Phys. Chem. A* **2006**, *110*, 7696.

(35) Amthor, S.; Lambert, C.; Dümmler, S.; Fischer, I.; Schelter, J. *J. Phys. Chem. A* **2006**, *110*, 5204.

(36) Demas, J. N.; Crosby, G. A. *J. Phys. Chem.* **1971**, *75*, 991–1024.

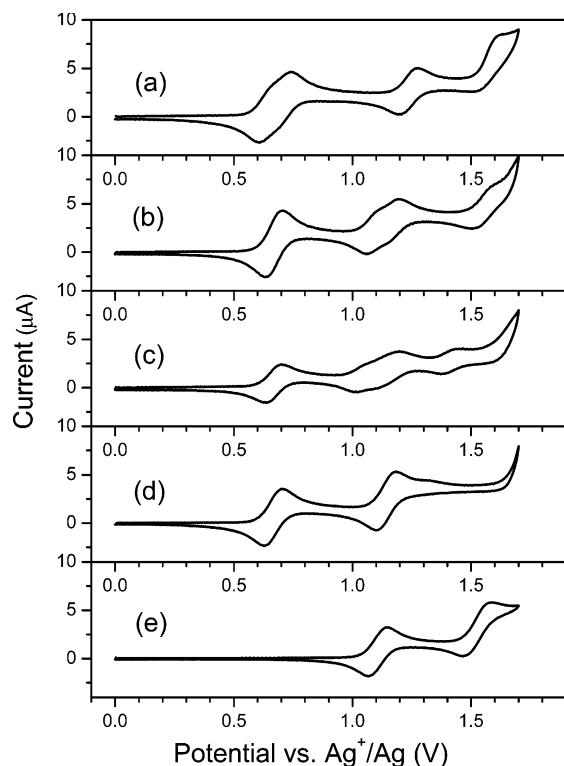


Figure 4. Cyclic voltammograms of compounds **1** (a), **2** (b), **3** (c), **4** (d), and **5** (e) in dichloromethane solutions.

Thin films of compounds **1–5** were fabricated by spin-casting their toluene solutions with the concentration of 20 mg/mL onto quartz substrates. Compared with the absorption and PL spectra of compounds **1–5** in toluene solutions, the absorption (Figure 2c) and PL spectra (Figure 3c) of the thin films of compounds **1–5** are almost identical, except that a 1–5 nm bathochromic shift was observed in their film spectra, probably due to the slight aggregation of the extended benzenoid system in their solid states.

Electrochemical Properties. The electrochemical behavior of the diamines **1–3** was investigated by cyclic voltammetry (CV) (Figure 4) and differential pulse voltammetry (DPV) (Figure 5), and all data are summarized in Table 2. The CV and DPV measurements were performed in a solution of Bu₄NPF₆ (0.1 M) in water-free dichloromethane with a scan rate of 50 mV/s at room temperature under argon. A platinum electrode was used as the working electrode and an Ag/Ag⁺ electrode as the reference electrode. For comparison, the CV and DPV of non- and monoarylamine-substituted pentaphenylenes **4** and **5** were also obtained under the same conditions, which facilitates the assignment of the individual redox waves. From the potential of the oxidation onset, the HOMOs of diamines **1–3** can be estimated to be around -4.9 eV according to eq 1,³⁷ and then the LUMOs of diamines **1–3** can be calculated to be around -2.2 eV by subtraction of the optical band gap (2.7 eV) from the $-E_{\text{HOMO}}$.

$$E_{\text{HOMO}} = -(E^{\text{ox}} + 4.34) \quad (1)$$

As shown in Figure 4a, diamine **1** displays four reversible one-electron anodic redox steps, which correspond to the

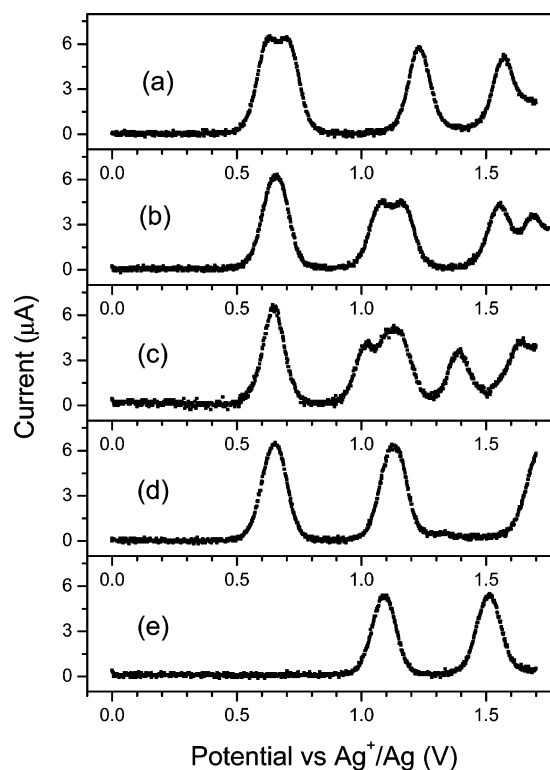


Figure 5. Differential pulse voltammograms of compounds **1** (a), **2** (b), **3** (c), **4** (d), and **5** (e) in dichloromethane solutions.

Table 2. Cyclic Voltammetry and Differential Pulse Voltammetry Data of Compounds **1–5** in Dichloromethane^a

compd	$E_{1/2}^1(\text{V})$	$E_{1/2}^2(\text{V})$	$E_{1/2}^3(\text{V})$	$E_{1/2}^4(\text{V})$	$E_{1/2}^5(\text{V})$
1	0.62 (1e)	0.72 (1e)	1.24 (1e)	1.56 (1e)	
2	0.67 (2e)	1.08 (1e)	1.18 (1e)	1.54 (1e)	1.68 (1e)
3	0.67 (2e)	1.04 (1e)	1.16 (2e)	1.40 (1e)	1.65 (1e or 2e)
4	0.67 (1e)	1.14 (1e)			
5	1.11 (1e)	1.52 (1e)			

^a 1e = one-electron transfer; 2e = two-electron transfer. Calculated from the integral of the DPV.

sequential removal of electrons from triarylamine and pentaphenylene moieties to form the stable radical cation, dication, trication, and tetracation. Compared with the CV of monoarylamine-substituted pentaphenylene **4** (Figure 4d), the first low-potential redox wave fits well with that of **4** ($E_{1/2}^1 = 0.67$ V), indicating that the first electron is removed from one of the triarylamine units. However, unlike one reversible redox couple found for compound **4**, diamine **1** shows two reversible redox processes in the low potential region at $E_{1/2}^1 = 0.62$ V and $E_{1/2}^2 = 0.72$ V, respectively, which means that the two electrons are removed successively from the two triarylamine moieties and a higher potential is needed to transform **1**^{•+} into **1**²⁺. This corresponds to a comproportionation constant of 49, according to eq 2,³⁸ and suggests diamine **1** to be a class II³⁹ derivative. Although electrochemical splittings have been often claimed

$$K_{\text{co}} = 10^{(\Delta E/0.059)} \quad (2)$$

as probes of delocalization in MV systems, the contribution of

(38) Richardson, D. E.; Taube, H. *Inorg. Chem.* **1981**, *20*, 1278.

(39) Robin, M.; Day, P. *Adv. Inorg. Radiochem.* **1967**, *10*, 247. Robin and Day distinguish among totally independent redox centers (class I), weakly or medium coupling (valence-trapped) redox centers (class II), and strongly coupling/completely delocalized centers (class III).

(37) Bard A. J.; Faulkner, L. A. *Electrochemical Methods—Fundamentals and Applications*; Wiley: New York, 1984.

electronic coupling to the comproportionation constant was shown to be small.⁴⁰ Thus, the electron coupling would contribute only ca. 5 mV to the comproportionation constant, while it is likely that the remaining 95 mV of the experimental splitting is largely due to Coulomb effects. Nevertheless, it is still not clear how the separations (largely determined by electrostatics) can be interpreted as evidence of delocalization. Correspondingly, the DPV of diamine **1** (Figure 5a) also displays two one-electron oxidations at 0.63 and 0.70 V. The splitting of the oxidations of two triarylamine units into two steps suggests effective charge delocalization through the conjugated ladder-type pentaphenylene in its MV radical monocation **1⁺** and long-distance electron communication between the two triarylamine branches. Compared with the CV and DPV spectra of pentaphenylene **5** without an arylamine unit, the third ($E_{1/2}^3 = 1.24$ V) and the fourth ($E_{1/2}^4 = 1.56$ V) reversible redox waves of diamine **1** correspond to the oxidation of the pentaphenylene unit into the radical cation and dication. However, small positive shifts for the third ($\Delta E_3 = 0.13$ V) and the fourth ($\Delta E_4 = 0.05$ V) redox waves suggest that the triarylamine units are positively charged and withdraw the electron density from the conjugated pentaphenylene systems.⁴¹

More interestingly, the first redox half-wave potential ($E_{1/2} = 0.67$ V) of diamine **2** (Figure 4b) is close to that of diamine **1**. However, in the case of the diamine **2**, the first redox couples cover two unresolved oxidation processes, indicating that the two electrons are almost simultaneously removed from the two triarylamines to form a dication. The corresponding DPV also shows only one two-electron oxidation process at 0.66 V. Neither electrostatic effects nor electron coupling could be observed due to the absence of electrochemical splitting, and the absence of electron coupling was further proved by chemical oxidation monitored by UV–vis–NIR absorption spectra. This is not surprising because the distance between the two redox centers is so large that they are definitely separated and behave independently. Another plausible explanation for the lack of electronic communication could invoke the pentaphenylene–pentaphenylene torsional junction. In contrast to the third redox wave of diamine **1**, the second oxidation processes of diamine **2** splits into two reversible redox processes at different potentials ($E_{1/2}^2 = 1.08$ V and $E_{1/2}^3 = 1.18$ V), and the redox waves are slightly shifted negatively ($\Delta E = -0.11$ V). With the increasing chain length of the oligopentaphenylenes, the first oxidation potential of the pentaphenylene shifts gradually to negative values and the number of possible redox processes successively increases because of the extension of the conjugated π system. This is a well-known behavior in homologous series of conjugated oligomers.⁴² Similarly, the DPV measurement (Figure 5b) also gave two oxidation peaks at $E = 1.08$ and 1.16 V ($\Delta E = 0.08$ V), which demonstrates that the electrons delocalize between the two pentaphenylene units and a weak electron coupling exists in the MV radical trication. In comparison to diamine **1**, the higher oxidation potential ($E_{1/2}^4 = 1.54$ V) of the pentaphenylene units also shifts to negative potentials ($\Delta E = -0.02$ V) due to the extended conjugation. However, with increasing number of pentaphenylene units, a resolved new redox wave appears in the higher potential region ($E_{1/2}^5 = 1.68$ V). The splitting of the oxidation ($\Delta E = 0.14$ V)

of diamine **2** into its pentacation **2⁵⁺** and hexacation **2⁶⁺** demonstrates an effective intervalence charge transfer between the pentaphenylene units.

The CV and DPV characterizations of the electrochemical properties of diamine **3** are shown in Figures 4c and 5c, respectively. Similar to diamine **2**, the first two-electron couples ($E_{1/2}^1 = 0.67$ V) can be assigned to the simultaneous oxidation of the two triarylamine branches, as explained above for diamine **2**, and there is no evidence for electronic communication between the two triarylamine centers because of the even longer distance. Due to the increased number of pentaphenylene units, the oxidation processes of pentaphenylene units became more complicated. As illustrated in Figure 5c, the first set of oxidation processes of the pentaphenylene system splits into a one-electron process ($E_{1/2}^2 = 1.04$ V) and a two-electron process ($E_{1/2}^3 = 1.16$ V), and the oxidation potentials of the oligopentaphenylene moieties shift slightly negatively ($\Delta E = -0.03$ V) with the same trend as found for diamine **2**. The two-step oxidation processes are also found in higher potential regions ($E_{1/2}^4 = 1.40$ V, $E_{1/2}^5 = 1.65$ V), with $\Delta E = 0.25$ V, and indicate a stronger electron coupling among the pentaphenylene units.

UV–Vis–NIR Absorption Spectra of Radical Cations. In order to further investigate the electronic communication behavior of the diamines **1–3**, chemical oxidation processes of diamines **1–3** in dichloromethane solutions (ca. 5×10^{-6} M) were performed, monitoring changes in their UV–vis–NIR absorption spectra with a stepwise addition of a $\text{SbCl}_5\text{--CH}_2\text{--Cl}_2$ solution (ca. 10^{-4} M). The corresponding spectral properties of the mono- and dications are shown in Figure 6a–d. For comparison, the chemical oxidation of monotriarylamine-substituted pentaphenylene **4** into its monocation **4⁺** was also performed, and the result is shown in Figure 6e.

As expected, the oxidation procedure of diamine **1** was divided into two subprocesses, as shown in Figure 6a,b. With the stepwise addition of 1 equiv of SbCl_5 , besides a normal band at $17\,700\text{ cm}^{-1}$, another very broad band appears in the NIR region at 5283 cm^{-1} (1893 nm), which is characteristic for an extended bridged triarylamine radical monocation and assigned to the intervalence charge transfer between the two redox triarylamine centers. The assignment of this long-wavelength absorption band in the NIR region is consistent with a previous report on the IVCT band.⁴³ However, unlike other IVCT systems with similar bridge length, the IVCT band of **1⁺** is very clear and intense. Furthermore, the molar extinction coefficients at $17\,700$ and 5283 cm^{-1} are almost the same ($\epsilon_{5283} = 15\,239\text{ M}^{-1}\text{ cm}^{-1}$). Upon further oxidation with 2 equiv of SbCl_5 , the NIR band at 5283 cm^{-1} completely disappears and the intensity of the band at $17\,700\text{ cm}^{-1}$ decreases a little, while an intense band at 7770 cm^{-1} , with a clear isosbestic point at 6270 cm^{-1} , increases continuously, obviously due to the triarylamine radical dication formation. For a more precise assignment of the triarylamine radical cation and dication bands, chemical oxidation with 1 equiv of SbCl_5 in dichloromethane was performed on monoamine **4**, a model compound in which there is only one triarylamine center and a triarylamine-to-triarylamine IVCT transition is impossible. A rather intense band was observed in the NIR region (7184 cm^{-1}), which corresponds to the electron transition from the highest bridge-based orbital

(40) Creutz, C. *Prog. Inorg. Chem.* **1983**, *30*, 1.

(41) Cremer, J.; Mena-Osteritz, E.; Pschierer, N. G.; Müllen, K.; Bäuerle, P. *Org. Biomol. Chem.* **2005**, *3*, 985.

(42) Heinze, J.; Tschuncky, P. *Electronic Materials: The Oligomer Approach*; Wiley-VCH: Weinheim, 1998.

(43) Lambert, C.; Nöll, G. *Chem. Eur. J.* **2002**, *8*, 3467.

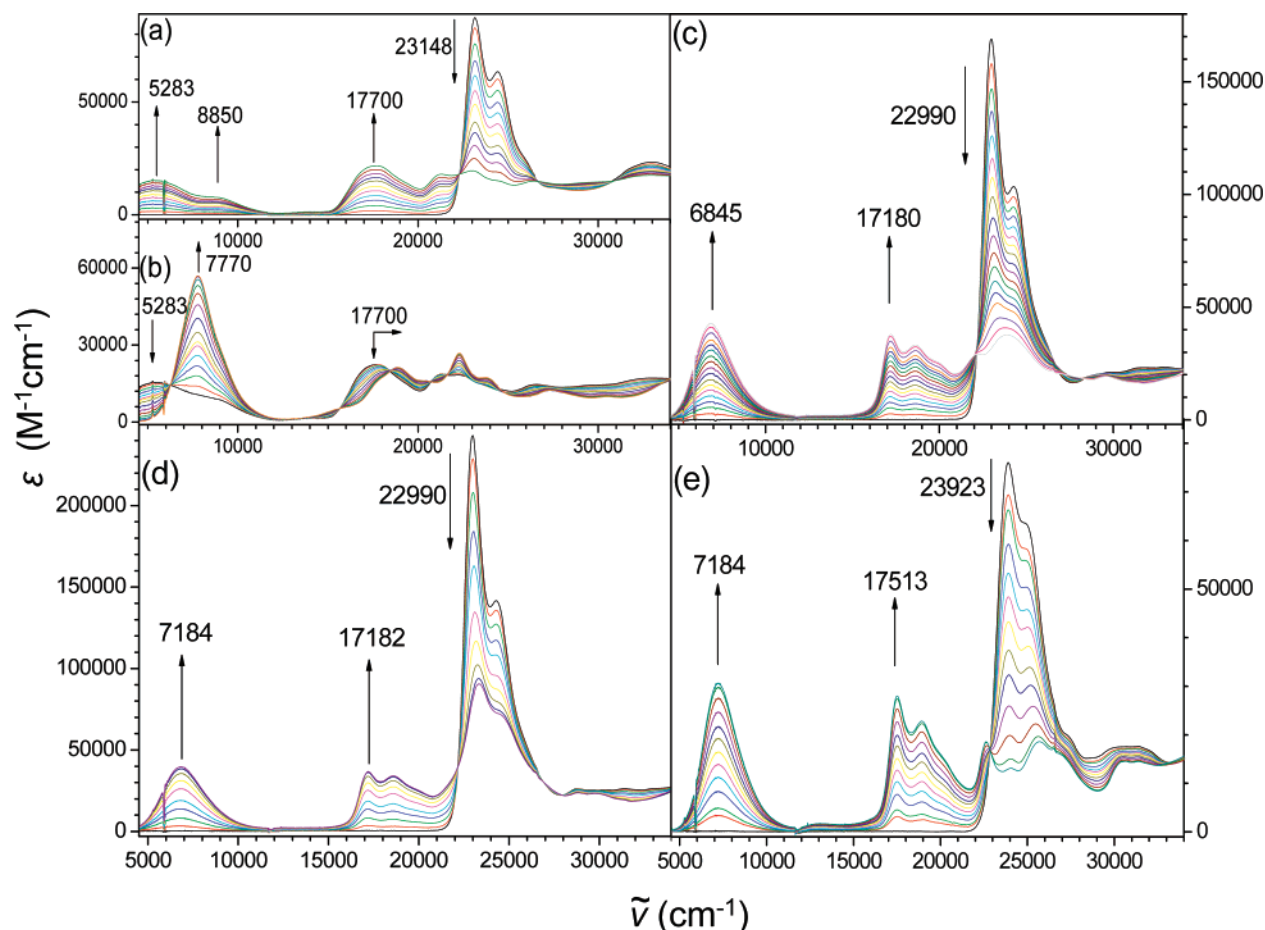


Figure 6. UV-vis-NIR absorption spectra of compounds **1** (a,b), **2** (c), **3** (d), and **4** (e) in dichloromethane solutions upon addition of SbCl_5 .

to the terminal redox center (bridge $\rightarrow \text{R}^+$).⁴⁴ The absorption spectrum of dication $\mathbf{1}^{2+}$ is similar to that of monocation $\mathbf{4}^+$ in the low-energy region with approximately twice the absorptivity, suggesting that the intense band at 7770 cm^{-1} of dication $\mathbf{1}^{2+}$ also originates from the charge transfer from the electron-rich and easily oxidized bridge to the donor radical cations. Moreover, higher energy transitions were observed at $17\,510 \text{ cm}^{-1}$, with a shoulder at $18\,940 \text{ cm}^{-1}$ and the decreasing band at $23\,920 \text{ cm}^{-1}$. The new absorption band is close to that of $[(p\text{-MeC}_6\text{H}_4)_3\text{N}]^+$ ($15\,000 \text{ cm}^{-1}$ in acetonitrile),⁴⁵ and the hypsochromic shift was also reported elsewhere,⁴⁴ which indicates that the higher energy absorption bands are assigned to the localized electron transitions from the HOMO to the LUMO.⁴⁶ The absorption shoulder at around $18\,940 \text{ cm}^{-1}$ is probably due to the 0–1 singlet transition, and the slight hypsochromic shift in the higher energy region observed upon going from $\mathbf{1}^+$ to $\mathbf{1}^{2+}$ could be ascribed to the changes of the electron energy levels between $\mathbf{1}^+$ and $\mathbf{1}^{2+}$.

The IVCT band found for $\mathbf{1}^+$ should be analyzed as is often done for CT compounds. According to Hush,⁴⁷ the electronic coupling can be calculated from the IVCT band maximum and

shape using eq 3,⁴⁸ where $\tilde{\nu}_{\text{max}}$ is the band energy in cm^{-1} , $\tilde{\nu}_{1/2}$

$$V = \frac{0.0206}{d} \sqrt{\tilde{\nu}_{\text{max}} \tilde{\nu}_{1/2} \epsilon} \quad (3)$$

is the bandwidth at half-height in cm^{-1} , ϵ is the molar extinction coefficient, and d in Å is taken as the distance between the two N atoms. $\tilde{\nu}_{\text{max}}$ is found to be 5283 cm^{-1} . Since the spectra could not be measured in a lower energy region, for crude estimation of the $\tilde{\nu}_{1/2}$ value, we assumed that the IVCT band was symmetrical and took the double dispersion from the IVCT band maximum to its half-height of the high-energy wavelength with the value of 4250 cm^{-1} . The electronic coupling energy V is then calculated to be 548 cm^{-1} (1.6 kcal/mol). This result is close to that for another reported IVCT compound, **C4**²⁵ (500 cm^{-1}), with a shorter bridge length (1.93 nm) but stronger donor (anisylamine), and demonstrates that diamine **1** can really be classified into class II,³⁹ as suggested already from eq 2. A problem in applying Hush's eq 3 is in determining the appropriate value of the diabatic electron-transfer distance, d .⁴⁴ In traditional inorganic MV systems, the metal–metal geometric separation is often used as an approximation, but in organic systems, there is more difficulty in defining the appropriate center of the charge-bearing unit. Especially when the conjugated bridge is electron-rich, the oxidation may not be centered

(44) (a) Barlow, S.; Risko, C.; Chung, S.-J.; Tucker, N. M.; Coropceanu, V.; Jones, S. C.; Levi, Z.; Brédas, J.-L.; Marder, S. R. *J. Am. Chem. Soc.* **2005**, *127*, 16900. (b) Rosokha, S. V.; Sun, D.-L.; Kochi, J. K. *J. Phys. Chem. A* **2002**, *106*, 2283.

(45) Walter, R. I. *J. Am. Chem. Soc.* **1966**, *88*, 1923.

(46) Zimmer, K.; Gödicke, B.; Hoppmeier, M.; Mayer, H.; Schweig, A. *Chem. Phys.* **1999**, *248*, 263.

(47) Hush, N. S. *Electrochim. Acta* **1968**, *13*, 1005.

(48) Creutz, C.; Newton, M. D.; Sutin, N. *J. Photochem. Photobiol. A* **1994**, *82*, 47.

exactly at the nitrogen atom but displaced somewhat into the bridge. Moreover, in both organic and inorganic cases, any delocalization of the charge away from the formal charge-bearing center toward the bridging group (for the diabatic states) will lead to reduced d . Thus, the value of V is likely to be a lower limit; i.e., the appropriate value of the diabatic electron-transfer distance is likely shorter than the N–N distance.

Figure 6c,d shows the evolution of absorption spectra of diamines **2** and **3** in dichloromethane solutions with the titration of SbCl_5 . However, quite different from the spectrum of diamine **1**, no IVCT band is observed when diamines **2** and **3** are chemically oxidized into monocations $2^{+\bullet}$ and $3^{+\bullet}$ with 1 equiv of SbCl_5 . Only “bridge \rightarrow $\text{R}^{+\bullet}$ ” transitions at around 7000 cm^{-1} were observed in the low-energy region, along with localized transitions of the arylamine monocation around $17\,180\text{ cm}^{-1}$. With further charging toward dications $2^{2+\bullet}$ and $3^{2+\bullet}$, the radical bands show almost double the absorbance of the mono-oxidized $2^{+\bullet}$ and $3^{+\bullet}$. This proves that the bridge distance is so long that the two triarylamine are absolutely isolated and the charge is localized at different redox centers. The absorption intensity of the neutral pentaphenylene at $22\,990\text{ cm}^{-1}$ in dication $3^{2+\bullet}$ is much higher than those for dications $1^{2+\bullet}$ and $2^{2+\bullet}$ due to a neutral central pentaphenylene unit.

Conclusions

In summary, a series of oligo(ladder-type pentaphenylene)s **1–5**, with or without ending bis(*p*-tolyl)amine substituents, has been designed and synthesized. The key intermediate is a monobromide-functionalized pentaphenylene **9**, obtained in moderate yields by an alternative two-step approach which involves an asymmetrical Buchwald coupling and an Ullmann-type arylation. Compared with the PL spectra of compounds **1–4** in toluene solutions, the PL spectra in dichloromethane solutions exhibit a 20–24 nm bathochromic shift due to the solvent-induced polarized excited states. The CV spectrum of diamine **1** shows a resolved splitting of oxidation with $\Delta E = 0.10\text{ V}$, corresponding to the stepwise oxidation of the two arylamines into $1^{+\bullet}$ and $1^{2+\bullet}$. Chemical oxidation of diamine **1** by SbCl_5 in dichloromethane solution reveals a broad IVCT band around 5283 cm^{-1} (1893 nm) which disappears upon further oxidation of $1^{+\bullet}$ into $1^{2+\bullet}$. Thus, a charge-transfer band indicating the hopping between the two arylamine centers was found only for compound **1**. No electronic communication between the two arylamine moieties was observed in diamines **2** and **3**. Here, the distances between the two arylamine centers in diamine **1** is comparable to that of the long phenylene ethynylene bridges used by Lambert et al. for studying intramolecular charge transfer. However, in their two cases, the bridge lengths of compounds **C4**²⁵ and **C5**²⁶ were 1.93 and 2.87 nm, respectively, and the IVCT bands were so weak that they could only be observed as small shoulders on the outer rings of the cation absorption spectra. Only for a much shorter diphenylacetylene bridge between the two arylamines, such as compound **C3**⁴⁹ with a bridge length of 1.25 nm, were similar intense IVCT bands reported. There, as here, the intensity of the NIR bands reaches an intensity comparable with those of the cation bands in the visible region. The relatively higher electronic coupling energy in MV cation $1^{+\bullet}$ can probably be ascribed to the more planar ladder-type pentaphenylene spacer than phe-

nylene ethynylene, which results in a better electron delocalization. Moreover, the electron coupling and hopping may be different if anisylamine instead of tolylamine groups are used due to the better charge localization at the triarylamine, and this will be discussed in our future work. Furthermore, we also have a stable bridge which can be reversibly charged up to the tetracation for diamine **1**, hexacation for **2**, and octacation for **3**. These findings provide evidence for long π -bridging, still allowing effective charge transfer between the redox centers with bridge lengths of 5–10 phenylene rings. Ongoing work is focused on their other optoelectronic applications, such as LED and two-photon absorption studies.

Experimental Section

All chemicals and reagents were used as received from commercial sources without further purification. Solvents for chemical synthesis were purified or freshly distilled prior to use according to standard procedures. All chemical reactions were carried out under an inert atmosphere. Intermediate ladder-type pentaphenylene **5** and dibromo-functionalized pentaphenylene **6** were synthesized according to previous work in our group.²⁷ ^1H and ^{13}C NMR spectra were recorded on a Bruker AMX 300 NMR instrument (300 and 75 MHz, respectively) with dichloromethane-*d* as solvent and tetramethylsilane as internal standard. The UV–vis–NIR absorption measurements were performed on a Perkin-Elmer Lambda 15 spectrophotometer, and the PL measurements on a SPEX Fluorolog 2 type F212 steady-state fluorometer. Cyclic voltammetry and differential pulse voltammetry were performed on an EG&G Princeton Applied Research potentiostat, model 273, in a solution of Bu_4NPF_6 (0.1 M) in dry dichloromethane with a scan rate of 50 mV/s at room temperature under argon. A platinum electrode was used as the working electrode, an Ag/AgCl electrode as the reference electrode, and a platinum wire as the counter electrode.

Synthesis of Compound 7. Under nitrogen atmosphere, a mixture of **6** (895 mg, 0.5 mmol), *p*-toluidine (161 mg, 1.5 mmol), $\text{Pd}(\text{OAc})_2$ (11 mg, 0.05 mmol), bis[2-(diphenylphosphino)phenyl] ether (DPEphos) (54 mg, 0.1 mmol), and sodium *tert*-butoxide (144 mg, 1.5 mmol) in toluene (50 mL) was stirred and heated at 80 °C for 8 h. After the reaction solution cooled to room temperature, a saturated ammonium chloride solution was added. The solution was extracted with ethyl acetate, and the extract was washed with brine and dried over magnesium sulfate. The crude product obtained was purified by flash column chromatography (silica gel, dichloromethane/hexane = 0 to 1/15 v/v). A yellowish solid was obtained with a yield of 85% (780 mg). ^1H NMR (300 MHz, CD_2Cl_2): δ (ppm) 7.68 (s, 2H), 7.54 (s, 2H), 7.45 (s, 2H), 7.39 (s, 1H), 7.35 (s, 1H), 7.16 (d, 8H, $J = 7.8\text{ Hz}$), 7.02 (d, 8H, $J = 8.4\text{ Hz}$), 6.98–6.84 (m, 10H), 6.81 (d, 2H, $J = 8.4\text{ Hz}$), 5.72 (s, 2H), 2.51 (t, 8H, $J = 7.5\text{ Hz}$), 2.20 (s, 6H), 1.88 (m, 8H), 1.50 (m, 8H), 1.21–1.11 (m, 40H), 1.05–0.99 (m, 40H), 0.79–0.68 (m, 24H), 0.62 (m, 8H). ^{13}C NMR (75 MHz, CD_2Cl_2): δ (ppm) 153.21, 152.30, 151.73, 150.62, 144.14, 143.49, 141.86, 141.71, 141.12, 140.44, 138.66, 134.46, 130.94, 130.24, 128.74, 128.65, 120.84, 118.59, 117.53, 116.38, 114.79, 112.08, 64.78, 41.17, 35.95, 32.32, 32.25, 31.96, 30.52, 29.96, 29.89, 29.77, 29.67, 24.41, 23.10, 23.03, 20.80, 14.32. MALDI-TOF: m/z 1841.7. Elemental Analysis for $\text{C}_{136}\text{H}_{180}\text{N}_2$, calculated: C, 88.64; H, 9.84; N, 1.52. Found: C, 88.68; H, 9.62; N, 1.38.

Synthesis of Diamine 1. To a 100 mL Schlenk flask containing **7** (450 mg, 0.24 mmol), *p*-iodotoluene (262 mg, 1.2 mmol), 1,10-phenanthroline (6 mg, 0.03 mmol), cuprous chloride (3 mg, 0.03 mmol), and potassium hydroxide (560 mg, 10 mmol), using argon as the purge gas and a Dean–Stark trap under a reflux condenser, was added 60 mL of toluene. The reaction mixture was refluxed at 140 °C for 24 h and quenched with acetic acid. After cooling to room temperature, the solution was extracted with ethyl acetate, washed with ammonia and water, and then dried by magnesium sulfate. After evaporation of the solvent under vacuum, the residue was purified by flash column

(49) Lambert, C.; Nöll, G. *Angew. Chem., Int. Ed.* **1998**, *37*, 2107.

chromatography (silica gel) using cyclohexane as eluent. A yellow solid was obtained with a yield of 70% (346 mg). ^1H NMR (300 MHz, CD_2Cl_2): δ (ppm) 7.68 (s, 2H), 7.53 (s, 2H), 7.45 (s, 2H), 7.35 (s, 1H), 7.32 (s, 1H), 7.15 (d, 8H, $J = 8.4$ Hz), 7.02 (d, 10H, $J = 8.1$ Hz), 6.97 (d, 10H, $J = 7.8$ Hz), 6.88 (d, 8H, $J = 6.9$ Hz), 2.47 (t, 8H, $J = 7.5$ Hz), 2.21 (s, 12H), 1.82 (m, 8H), 1.50 (m, 8H), 1.22–1.17 (m, 40H), 1.12–0.98 (m, 40H), 0.80–0.71 (m, 24H), 0.60 (m, 8H). ^{13}C NMR (75 MHz, CD_2Cl_2): δ (ppm) 152.76, 152.30, 151.72, 144.01, 141.83, 140.40, 132.52, 130.24, 130.10, 129.91, 128.68, 128.58, 124.77, 124.44, 124.37, 124.25, 124.18, 124.14, 118.66, 117.55, 116.70, 114.77, 64.72, 40.89, 35.88, 32.26, 32.21, 31.89, 30.40, 30.07, 29.89, 29.82, 29.70, 29.61, 24.36, 23.04, 23.00, 20.84, 14.25. MALDI-TOF: m/z 2023.7. Elemental analysis for $\text{C}_{150}\text{H}_{192}\text{N}_2$, calculated: C, 89.05; H, 9.57; N, 1.38. Found: C, 89.25; H, 9.61; N, 1.34.

Synthesis of Compound 8. Under nitrogen atmosphere, a mixture of **6** (1.79 g, 1.0 mmol), *p*-toluidine (128 mg, 1.2 mmol), $\text{Pd}(\text{OAc})_2$ (23 mg, 0.1 mmol), DPEphos (107 mg, 0.2 mmol), and sodium *tert*-butoxide (144 mg, 1.5 mmol) in toluene (50 mL) was stirred and heated at 80 °C for 8 h. After the reaction solution cooled to room temperature, saturated ammonium chloride solution was added. The solution was extracted with ethyl acetate, and the extract was washed with brine and dried over magnesium sulfate. The crude product was subjected to flash column chromatography (silica gel, dichloromethane/hexane = 0 to 1/15 v/v). A yellowish solid was obtained with a yield of 35% (635 mg). ^1H NMR (300 MHz, CD_2Cl_2): δ (ppm) 7.71 (s, 1H), 7.69 (s, 1H), 7.57 (s, 1H), 7.54 (s, 2H), 7.45 (s, 1H), 7.41–7.30 (m, 4H), 7.17 (d, 8H, $J = 8.4$ Hz), 7.03 (d, 9H, $J = 8.1$ Hz), 6.95–6.91 (m, 3H), 6.84 (d, 1H, $J = 8.1$ Hz), 5.74 (s, 1H), 2.48 (t, 8H, $J = 7.8$ Hz), 2.21 (s, 3H), 1.88 (m, 8H), 1.50 (m, 8H), 1.27–1.17 (m, 40H), 1.11–0.99 (m, 40H), 0.79–0.68 (m, 24H), 0.59 (b, 8H). ^{13}C NMR (75 MHz, CD_2Cl_2): δ (ppm) 153.79, 153.19, 152.43, 152.31, 151.85, 151.73, 150.81, 150.61, 144.01, 143.85, 143.52, 141.93, 141.86, 141.04, 140.98, 140.64, 140.48, 140.16, 139.87, 138.42, 135.97, 134.32, 133.29, 130.95, 130.19, 130.11, 128.70, 128.59, 126.52, 121.37, 121.03, 118.66, 118.58, 118.51, 117.82, 117.53, 116.31, 114.85, 64.73, 41.10, 40.92, 35.88, 32.26, 32.18, 32.14, 31.90, 30.46, 30.34, 29.90, 29.83, 29.70, 29.61, 24.36, 24.22, 23.04, 22.97, 20.74, 14.25, 14.22. MALDI-TOF: m/z 1816.9. Elemental analysis for $\text{C}_{129}\text{H}_{172}\text{BrN}$, calculated: C, 85.29; H, 9.54; Br, 4.40; N, 0.77. Found: C, 85.28; H, 9.48; N, 0.74.

Synthesis of Compound 9. To a 100 mL Schlenk flask containing **8** (600 mg, 0.33 mmol), *p*-iodotoluene (218 mg, 1 mmol), 1,10-phenanthroline (6 mg, 0.03 mmol), cuprous chloride (3 mg, 0.03 mmol), and potassium hydroxide (560 mg, 10 mmol), using argon as the purge gas and a Dean–Stark trap under a reflux condenser, was added 60 mL of toluene. The reaction mixture was refluxed at 140 °C for 24 h and quenched with acetic acid. After cooling to room temperature, the solution was extracted with ethyl acetate, washed with ammonia and water, and then dried by magnesium sulfate. After evaporation of the solvent under vacuum, the residue was purified by flash column chromatography (silica gel) with petroleum ether as eluent. A yellow solid was obtained with a yield of 83% (520 mg). ^1H NMR (300 MHz, CD_2Cl_2): δ (ppm) 7.71 (s, 1H), 7.69 (s, 1H), 7.57 (s, 1H), 7.54 (s, 2H), 7.46 (s, 1H), 7.40–7.29 (m, 4H), 7.15 (d, 8H, $J = 7.5$ Hz), 7.02 (d, 8H, $J = 8.1$ Hz), 6.96 (d, 5H, $J = 8.4$ Hz), 6.87 (d, 4H, $J = 8.4$ Hz), 6.78 (d, 1H, $J = 8.1$ Hz), 2.47 (t, 8H, $J = 7.5$ Hz), 2.20 (s, 6H), 1.91 (m, 4H), 1.79 (m, 4H), 1.49 (m, 8H), 1.21–1.16 (m, 40H), 1.11–0.97 (m, 40H), 0.79–0.68 (m, 24H), 0.60 (b, 8H). ^{13}C NMR (75 MHz, CD_2Cl_2): δ (ppm) 153.80, 152.78, 152.48, 152.37, 151.88, 151.79, 151.07, 150.83, 147.96, 146.00, 143.98, 143.85, 141.95, 141.89, 141.57, 140.91, 140.65, 140.47, 140.22, 139.99, 138.81, 137.58, 135.78, 132.54, 131.61, 130.12, 128.75, 128.72, 128.58, 126.52, 124.40, 121.39, 121.08, 120.50, 118.63, 117.86, 117.58, 116.73, 64.75, 40.91, 35.90, 32.28, 32.24, 32.16, 31.92, 30.42, 30.37, 29.91, 29.85, 29.73, 29.63, 24.37, 24.23, 23.06, 23.03, 22.98, 20.88, 14.28, 14.24. MALDI-TOF: m/z 1905.8. Elemental analysis for $\text{C}_{136}\text{H}_{178}\text{BrN}$, calculated: C, 85.67; H, 9.41; Br, 4.19; N, 0.73. Found: C, 85.85; H, 9.16; N, 0.77.

Synthesis of Compound 4. Under nitrogen atmosphere and at -78 °C, *n*-BuLi (0.1 mL, 1.6 M in hexane) was added dropwise to a dry tetrahydrofuran (20 mL) solution containing **9** (240 mg, 0.13 mmol). After the reaction solution was stirred for 10 min at -78 °C, 0.1 mL of saturated brine was added slowly. The solution was brought back to room temperature, and after being stirred for another 4 h, the reaction was quenched by brine. The solution was extracted with ethyl acetate, and the extract was washed with brine and dried over magnesium sulfate. The crude product was subjected to flash column chromatography (silica gel, petroleum ether). Compound **4** was obtained as a yellow powder with a yield of 93% (215 mg). ^1H NMR (300 MHz, CD_2Cl_2): δ (ppm) 7.71 (s, 1H), 7.69 (s, 1H), 7.59 (s, 1H), 7.56 (s, 1H), 7.54 (s, 1H), 7.51 (m, 1H), 7.46 (s, 1H), 7.34 (d, 1H, $J = 8.1$ Hz), 7.24 (s, 1H), 7.16 (d, 10H, $J = 7.5$ Hz), 7.02 (d, 8H, $J = 8.1$ Hz), 6.96 (d, 5H, $J = 8.4$ Hz), 6.87 (d, 4H, $J = 8.4$ Hz), 6.78 (d, 1H, $J = 8.1$ Hz), 2.47 (t, 8H, $J = 7.8$ Hz), 2.20 (s, 6H), 1.92 (m, 4H), 1.79 (m, 4H), 1.50 (m, 8H), 1.21–1.16 (m, 40H), 1.11–0.96 (m, 40H), 0.79–0.67 (m, 24H), 0.60 (m, 8H). ^{13}C NMR (75 MHz, CD_2Cl_2): δ (ppm) 152.78, 152.43, 152.33, 151.77, 151.65, 151.49, 151.17, 151.05, 147.94, 146.02, 144.02, 141.87, 141.48, 141.40, 140.68, 140.26, 139.94, 138.91, 135.83, 132.53, 130.12, 128.72, 128.60, 127.23, 126.99, 125.81, 124.39, 124.34, 123.26, 122.70, 120.50, 119.95, 118.66, 117.77, 117.61, 117.43, 116.73, 114.93, 114.84, 64.76, 41.02, 40.93, 35.91, 32.29, 32.25, 32.18, 31.93, 30.50, 30.44, 29.92, 29.85, 29.74, 29.64, 24.38, 24.30, 23.07, 23.03, 22.98, 20.89, 14.29, 14.24. MALDI-TOF: m/z 1827.4. Elemental analysis for $\text{C}_{136}\text{H}_{179}\text{N}$, calculated: C, 89.36; H, 9.87; N, 0.77. Found: C, 89.47; H, 9.65; N, 0.57.

Synthesis of Compound 10. Under nitrogen atmosphere and at -78 °C, *n*-BuLi (0.43 mL, 1.6 M in hexane) was added dropwise to a dry tetrahydrofuran (20 mL) solution containing **9** (1.20 g, 0.63 mmol). After the reaction solution was stirred for 30 min at -78 °C, 0.25 mL (1.2 mmol) of 2-isopropoxy-4,4,5,5-tetramethyl-1,3,2-dioxaborolane was added slowly. The solution was brought back to room temperature, and after being stirred for another 24 h, the reaction was quenched with brine. The solution was extracted with ethyl acetate, and the extract was washed with brine and dried over magnesium sulfate. The crude product was separated by flash column chromatography (silica gel, dichloromethane/hexane = 0 to 1/5 v/v). Compound **10** was obtained as a yellow powder with a yield of 29% (230 mg). ^1H NMR (300 MHz, CD_2Cl_2): δ (ppm) 7.73 (s, 1H), 7.70 (s, 1H), 7.60 (d, 2H, $J = 6.9$ Hz), 7.53 (d, 2H, $J = 6$ Hz), 7.46 (s, 2H), 7.36 (s, 1H), 7.33 (s, 1H), 7.16 (d, 8H, $J = 8.1$ Hz), 7.02 (d, 8H, $J = 7.8$ Hz), 6.97 (d, 5H, $J = 8.4$ Hz), 6.87 (d, 4H, $J = 8.7$ Hz), 6.78 (d, 1H, $J = 8.1$ Hz), 2.48 (t, 8H, $J = 7.8$ Hz), 2.22 (s, 6H), 1.94 (m, 4H), 1.82 (m, 4H), 1.50 (m, 8H), 1.27 (s, 12H), 1.20–1.17 (m, 40H), 1.08–0.98 (m, 40H), 0.80–0.67 (m, 24H), 0.60–0.57 (m, 8H). ^{13}C NMR (75 MHz, CD_2Cl_2): δ (ppm) 161.97, 159.06, 151.61, 151.15, 150.61, 150.52, 149.47, 147.84, 144.84, 142.82, 142.77, 140.74, 140.71, 140.22, 131.95, 131.37, 128.94, 127.53, 127.42, 125.14, 123.21, 122.42, 121.52, 116.71, 116.42, 112.67, 103.56, 100.37, 99.25, 93.84, 93.38, 92.92, 82.90, 63.58, 34.73, 31.11, 31.06, 30.99, 30.74, 29.25, 28.74, 28.67, 28.55, 28.46, 28.41, 23.98, 21.89, 21.85, 21.80, 19.70, 13.10. FD-MASS: m/z 1953.2.

Synthesis of Diamine 2. A solution of bis(1,5-cyclooctadiene)nickel (100 mg, 0.36 mmol), 2,2'-bipyridine (60 mg, 0.38 mmol), and 1,5-cyclooctadiene (0.05 mL, 0.4 mmol) was dissolved in dry toluene (4 mL) and dry *N,N*-dimethylformamide (4 mL) in a Schlenk flask within a glovebox. The mixture was heated to 60 °C with stirring under argon for 30 min. A solution of bromide **9** (570 mg, 0.30 mmol) in 8 mL of dry toluene was then added, and the reaction mixture was stirred at 80 °C for 2 days. After cooling to room temperature, the reaction mixture was poured into chloroform and washed with water and brine. The separated organic layer was dried over magnesium sulfate, and the solvent was evaporated. Chromatography of the crude product on silica gel with cyclohexane as eluent gave diamine **2** as a yellow powder (405 mg, 74%). ^1H NMR (300 MHz, CD_2Cl_2): δ (ppm) 7.73 (s, 2H), 7.70 (s, 2H), 7.61 (d, 4H, $J = 4.8$ Hz), 7.58 (s, 2H), 7.55 (s, 5H), 7.51

(s, 1H), 7.47 (s, 2H), 7.36 (s, 1H), 7.33 (s, 1H), 7.18 (d, 8H, $J = 8.4$ Hz), 7.16 (d, 8H, $J = 5.4$ Hz), 7.04 (d, 8H, $J = 8.4$ Hz), 7.03 (d, 8H, $J = 8.4$ Hz), 6.96 (d, 10H, $J = 8.4$ Hz), 6.88 (d, 8H, $J = 8.4$ Hz), 6.78 (d, 2H, $J = 7.5$ Hz), 2.49 (t, 16H, $J = 7.8$ Hz), 2.21 (s, 12H), 2.00 (m, 8H), 1.80 (m, 8H), 1.53–1.46 (m, 16H), 1.22–1.17 (m, 80H), 1.09–0.99 (m, 80 H), 0.79–0.62 (m, 64H). ^{13}C NMR (75 MHz, CD_2Cl_2): δ (ppm) 152.77, 152.45, 152.34, 152.26, 151.76, 151.52, 151.05, 147.95, 146.10, 146.07, 146.02, 145.99, 144.01, 143.98, 141.91, 141.87, 141.48, 141.10, 140.72, 140.56, 140.24, 139.97, 138.89, 135.85, 135.80, 132.53, 130.12, 128.72, 128.61, 126.21, 124.39, 122.74, 122.70, 121.63, 120.24, 118.65, 117.77, 117.60, 117.47, 116.73, 114.99, 114.85, 64.77, 41.05, 40.91, 35.90, 32.28, 32.23, 32.15, 31.92, 30.42, 29.91, 29.85, 29.72, 29.63, 24.37, 24.29, 23.06, 23.02, 22.96, 20.87, 14.27, 14.22. MALDI-TOF: m/z 3655.3. Elemental analysis for $\text{C}_{272}\text{H}_{356}\text{N}_2$, calculated: C, 89.41; H, 9.82; N, 0.77. Found: C, 89.29; H, 9.73; N, 0.70.

Synthesis of Diamine 3. The dibromopentaphenylene **6** (90 mg, 1 mmol) and boronate ester **10** (220 mg, 3 mmol) in toluene (25 mL) and 2 M aqueous Na_2CO_3 solution (25 mL) were mixed together in a 100 mL Schlenk flask. The solution was purged with argon for 20 min, 6 mg (10% mol) of tetrakis(triphenylphosphine)palladium was added, and the reaction was heated at 85 °C for 48 h. The cooled mixture was extracted with ethyl acetate, and the extract was washed with saturated brine and then dried over magnesium sulfate. After removal of the solvent, the residue was purified by column chromatography using cyclohexane as eluent. The diamine **3** was isolated as a yellow powder (130 mg, 49%). ^1H NMR (300 MHz, CD_2Cl_2): δ (ppm) 7.75 (s, 2H),

7.73 (s, 2H), 7.70 (s, 2H), 7.63–7.51 (m, 21H), 7.46 (s, 2H), 7.36 (s, 1H), 7.33 (s, 1H), 7.21–7.15 (m, 25H), 7.06–7.01 (m, 25H), 6.97 (d, 11H, $J = 8.4$ Hz), 6.87 (d, 9H, $J = 8.4$ Hz), 6.79 (d, 2H, $J = 8.1$ Hz), 2.49 (t, 24H, $J = 7.2$ Hz), 2.21 (s, 12H), 2.00 (b, 8H), 1.82 (b, 4H), 1.80, 1.51 (m, 24H), 1.22–1.17 (m, 120H), 1.12–0.99 (m, 120H), 0.79–0.63 (m, 96H). ^{13}C NMR (75 MHz, CD_2Cl_2): δ (ppm) 152.76, 152.47, 152.44, 152.32, 152.25, 151.78, 151.75, 151.51, 151.04, 147.91, 145.99, 144.00, 143.96, 141.93, 141.90, 141.86, 141.46, 141.17, 141.08, 140.69, 140.52, 140.23, 139.96, 139.89, 138.88, 135.81, 132.52, 131.79, 130.10, 128.74, 128.60, 126.21, 124.37, 122.68, 121.62, 120.49, 120.25, 120.21, 117.78, 117.47, 116.71, 64.76, 41.05, 40.92, 35.89, 32.26, 32.22, 32.14, 32.03, 31.91, 30.41, 30.08, 29.90, 29.83, 29.71, 29.61, 24.35, 24.27, 23.04, 23.00, 22.95, 20.85, 14.25, 14.20. MALDI-TOF: m/z 5283.0. Elemental analysis for $\text{C}_{394}\text{H}_{520}\text{N}_2$, calculated: C, 89.55; H, 9.92; N, 0.53. Found: C, 89.30; H, 9.82; N, 0.49.

Acknowledgment. This work was financially supported by the Bundesministerium für Bildung und Forschung (Projects 13N8165 OLAS and 13N8215 OLED) and by Dupont Displays. G.Z. gratefully acknowledges the Alexander von Humboldt Stiftung for the grant of a research fellowship.

Supporting Information Available: ^1H NMR spectra of compounds **1–10**. This material is available free of charge via the Internet at <http://pubs.acs.org>.

JA073148S